Nigerian Journal of Physics (NJP)
ISSN online: 3027-0936
ISSN print: 1595-0611
DOI: https://doi.org/10.62292/njp.v33(s).2024.264
Volume 33(S) 2024

Velocity Anisotropy: Temperature Effect on Thomson's Parameter of Ogun Shale, Ogun State, Nigeria

[1]Kuforiji, H. I., *[2]Bello, R., [3]Abatan, A. O. and [4]Akinyemi, O. D.

[1]Deparment of Physical Sciences, Al-hikmah University, Ilorin, Kwara State, Nigeria
[2]Department of Physics, Federal University of Kashere, Gombe state, Nigeria
[3]Department of SLT, Moshood Abiola Polytechnic, Abeokuta Ogun State, Nigeria
[4]Department of Physics, Federal University of Agriculture, Abeokuta, Nigeria

*Corresponding author's email: bellomo75@gmail.com

ABSTRACT

When a rock's physical property is directional or orientation-dependent, the rock is described as being anisotropic. Shale is a common sedimentary rock with inherent anisotropic nature gotten from its geological evolution. Thus in studying the elastic properties of shale, the direction of the wave propagation has to be considered and reported. Velocity anisotropy of shale with temperature effect on the Thomson's anisotropic parameters was carried out on shales from Ogun state in the southwestern part of Nigeria. Ultrasonic velocity measurement was carried out at temperatures ranging between 50 and 300 ˚C. Elastic properties, as well as the anisotropic parameters were determined. The parameters were compared with the temperature and elastic properties of the samples. Results showed that Ogun state shales are anisotropic and that both P and S wave pulses exhibited higher values in the horizontal direction (along the bedding plane) than in the vertical orientation (normal to the bedding plane) of the samples. Elastic modulus was higher in the horizontal direction while the Poisson's ratio and velocity ratio were higher in the vertical plane. Anisotropic parameters, gamma (ϒ) and epsilon (Ɛ) exhibited value reduction up to about 150 ˚C when they started to increase with increasing temperature. Gamma however increased more notably than the epsilon. This result indicated that fractures and microcracks within the shale samples closed up as the samples expanded due to temperature increase.

Keywords:
Anisotropy,
Elastic Modulus,
Poisson's Ratio,
Shale,
Thompson Parameters,
Ultrasonic Velocity.

INTRODUCTION

Shales are laminated sedimentary rocks considered to be complex rocks due to their mechanical anisotropy (Sone and Zoback, 2013; Johnston, 1987). The geological evolution of shale gives it the inherent anisotropic nature, which makes its elastic properties to be orientation dependent. During formation, transported silts and clay are deposited and become compacted by sediments above with the clay minerals and micas rearranged in a parallel manner to give the shale its laminated structure (Okeke and Okogbue, 2011; Johnston and Christensen, 1995; Sondergeld and Rai, 1993). Organic materials compliantly contribute to shale formation (Ahmadov *et al*., 2009; Kumar *et al*., 2012; Vernik and Milovac, 2011; Sondergeld *et al*., 2000). In the study of rocks, the anisotropy is an important factor that is capable of influencing properties of the rock. According to Sone and Zoback (2013), when anisotropy is well understood, seismic surveys, sonic logs, as well as microseismic monitoring could be easily analysed and interpreted.

While studying the anisotropy, it is very necessary to know the contributing effects of the physical conditions of the rock, which may include pressure, pore saturation, and temperature. The anisotropic nature of shale had been studied in several pieces of research (Jones and Wang, 1981, Tosoya and Nur, 1982; Vernik and Liu, 1997; Hornby, 1998; Jakobsen & Johansen, 2000; Domnesteanu *et al.*, 2002; Sone and Zoback, 2013; Douma *et al*., 2016; Takanashi *et al*., 2001; Wang and Li, 2017 and Xu et al., 2017) with most of the works emphasizing the pressure effects on the velocity anisotropy. Temperature is one of the factors that affect wave velocities of rocks (Kuforiji *et al*., 2021), the ultimate strength and elastic moduli of shales (Douma *et al*., 2016), the. The study, which investigated the

mechanical behavior of shales revealed that shale deformability is enhanced by an increase in temperature. Earlier, Waxman and Thomas (1974) reported that the resistivity of shale is affected by temperature. Shales could be very sensitive to temperature thereby having a very significant temperature coefficient. Huang *et al*,. (1995) concluded that shales developed higher swelling potential below the temperature of 0 ˚C, yet the temperature is the least controlling factor of the swelling of the media. The study however did not consider the anisotropy effect.

Ogun State shales are silty argillaceous (silt dominant) and near-surface. The recent increase in scientific researches on rock mechanics of shale in Ogun State southwestern Nigeria follows the industrial production of shale in the region, which has together with limestone and granite made Ogun State emerge several times (in 2019/2020) as the highest solid mineral producing state in Nigeria (NBS). Meanwhile, most of the available works on Ogun shales had studied several properties of the shales without necessarily considering the anisotropic effects knowing fully well that anisotropy is a major influential factor of many properties of rocks particularly the elastic properties. Takanashi *et al*., (2001) oblige that when dealing with seismic waves propagation through the crust, the effects of velocity anisotropy must be considered. Also, Dewhurst and Siggins (2006) submitted that significant error can be caused by anisotropy in the estimation of dynamic Poisson's ratio.

This paper studied the anisotropy of shale from Ogun State Nigeria at varying temperature and constant pressure conditions. The temperature was applied in steps of 50 up to 300 ˚C. The consequential effects of temperature increase on Thompson anisotropic parameters were focused on.

MATERIALS AND METHODS

The study area is Ogun state southwestern Nigeria, geographically located between latitude 6˚22′3.0008" and 7˚54′35.982" North and longitude 2˚44′14.2404" and 4˚35′37.2228" East. Ogun state is bordered in the north by Oyo state with an air travel (bird fly) distance of about 65 km from Ibadan, the Oyo state capital. In the south, the study area is bordered by Lagos state with a distance of 78 km from Ikeja, the capital of Lagos state. Ogun state shared international boundary with Benin republic to the West and with Ondo state to the east with a birds-fly distance of about 144 km. The geology of the state comprises Coastal plain sands, the Basement complex, Ilaro, Oshosun, Ewekoro, and Abeokuta formations. The formations are part of the component formations of the Nigerian sector of the Dahomey basin, which stretches from the Volta River in Ghana, extends from Nigeria's boundary with the Benin Republic to the Benin Hinge line (Petters and Richard, 1979) (Figure 1). Oshosun formation is overlain by Ilaro formation with the embayment axes as well as its thickness slightly occurring west of the Nigerian border with the Benin Republic. Limestone and shale (black and grey) are the main lithologic units in the Oshosun and Ilaro formations. The stratigraphy of the formation showed that red clay overlay the shale, which in turn overlay the limestone. In some parts of the Ibese axis of the formation, the topsoil and the red clay overlay the shale to a depth of five to ten meters. There is no doubt that Ogun state is a major solid mineral producing state in Nigeria. The results of laboratory studies on the rocks continue to attract more investors in quarrying businesses in the state. In recent time, researcher from within and outside Ogun state have presented many works on the rock components of the state geology especially in the area of characterization. In most of these works however, it is observed that less attention has been given to the anisotropic properties of some of the rocks studied in the state. Hence the need for the study in the state.

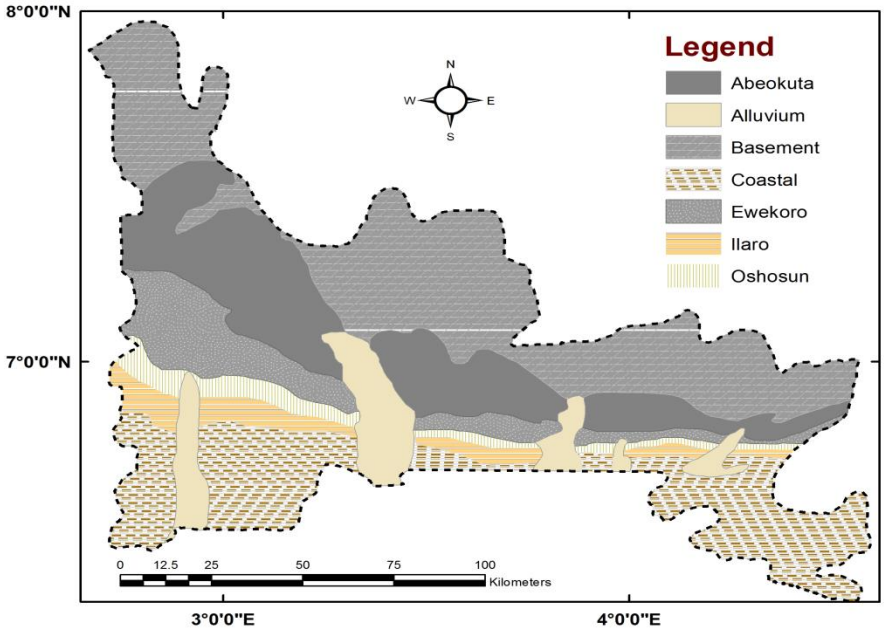

Figure 1: Map of Ogun state showing the geology of the state

Shale samples were collected as a regular cube of dimension L × B × H, with the bedding plane of the shale parallel to the surface L × B after which the samples were oven-dried at 105 ˚C for twenty-four hours. Clean pulverized samples were prepared for XRD analysis while other small crystal samples were carefully cut for photomicroscopy. Both analyses were carried out at the Nigerian Geological Survey Agency, Kaduna Nigeria. Velocities of the compressional and shear waves propagating through the shale cubes were measured using an ultrasonic pulse transmission technique. For geologic materials, elastic constants are commonly determined by pulse transmission methods (Wang and Li, 2017; Anil and Anirbid 2014; Brahma and Sircar, 2014; Ji-Xin *et al*., 2004). The measurements were done using Proceq (CT-135 Pundit Lab, using ASTM D 2845 standard method), which was coupled to a heating gadget. The transit time of the machine ranges from 0.1 to 9999 μs and has a resolution of 0.1 μs. The frequency ranges between 24 and 500 kHz. A thermocouple thermometer was embedded in the sampler to monitor the temperature of the system.

Temperature was applied in steps of 50 up to 300 ˚C and each time the required temperature is attained, the system was regulated to maintain the temperature for the next five minutes to ensure uniform heating of the sample. The energy was first transmitted into uniformly heated shale cube (in a direction parallel to the bedding planes or normal to the symmetry axis) at 50 ˚C while the velocities of both the compressional and shear waves parallel to the bedding plane were measured. The orientation of the transducers was quickly changed to measure the velocities of the compressional and shear waves perpendicular to the bedding planes. The heating continued after the measurements until the next required temperature (100 ˚C) at which the measurements were again done and the processes continued till the last required temperature (300 ˚C). Importantly, the machine was preset to take the measurements ten times in each case after which the average values were then calculated and recorded. This becomes necessary as the ultrasonic velocity measurement (at lower pressure) requires this.

Theory

During a measurement, the sender transducer emits the energy into the rock, which upon reaching the receiver transducer is converted back to an electrical signal to determine the travel time (t) of the wave pulse. Thus the only input data required is the traveling path length (d), which is automatically used together with the travel time to calculate the wave velocity according to Equation 1.

$$V = \frac{d}{t} \quad (1)$$

At a preset constant time interval, the machine measures the compressional (P-wave) and shear wave (S-wave) velocities and automatically stores the data including the waveform. The 250 kHz shear wave transducers were used since the P-wave component is also present in this type of transducer (Figure 2). When the predetermined density (ρ) of the sample under test is imputed to the machine, both the Poisson's ratio and elastic modulus can be obtained by the machine respectively according to Equations 2 and 3. Elastic properties and Thompson

anisotropic parameters could also be calculated using the dynamic approach (Xu *et al*., 2016).

$$v = \frac{V_P^2 - 2V_S^2}{2(V_P^2 - V_S^2)} \quad (2)$$

$$E = 2G(1 + v) \quad (3)$$

where v is the Poisson's ratio
V_P is the compressional wave velocity
V_S is the shear wave velocity
E is the elastic modulus
G is the shear wave modulus given as:

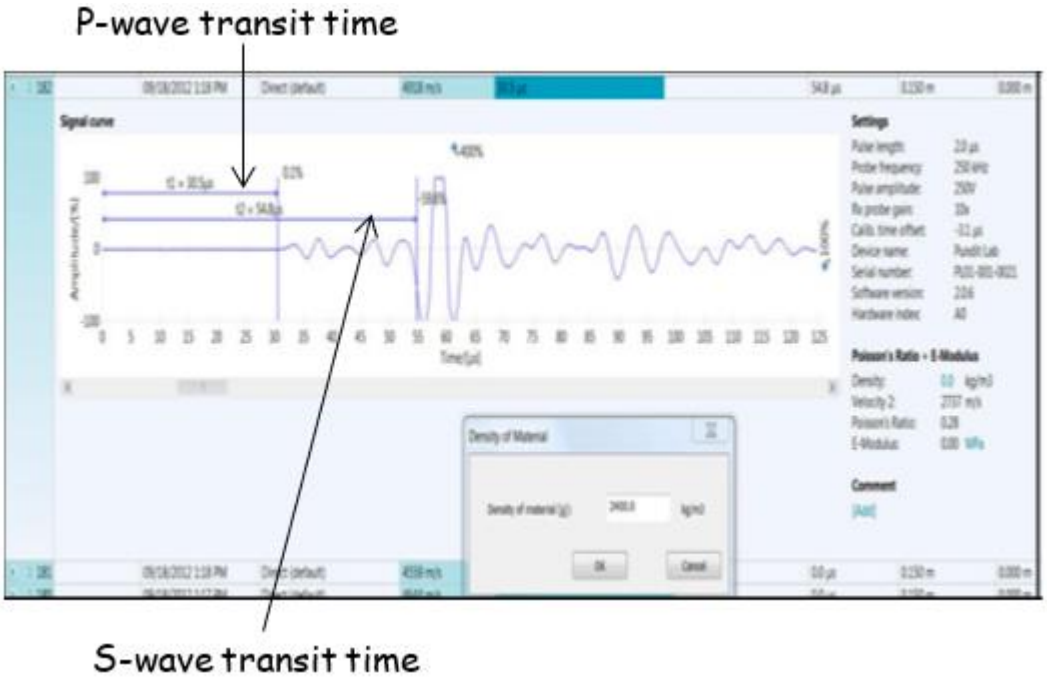

Figure 2: P and S wave travel time measurement (Proceq, 2011)

$$G = \rho V_S^2 \quad (4)$$

Anisotropic parameters are given as equations 5 and 6

$$\varepsilon = \frac{C_{11} - C_{33}}{2C_{33}} \quad (5)$$

$$\gamma = \frac{C_{66} - C_{44}}{2C_{44}} \quad (6)$$

where C_{11}, C_{33}, C_{44} and C_{66} are stiffness constants.

$$\propto_{\perp}^2 = \frac{C_{33}}{\rho} \quad (7)$$

$$\beta_{\perp}^2 = \frac{C_{44}}{\rho} \quad (8)$$

$$\propto_{=}^2 = \frac{C_{11}}{\rho} \quad (9)$$

$$\beta_{=}^2 = \frac{C_{66}}{\rho} \quad (10)$$

$\propto_{\perp}$ is the P-wave velocity perpendicular to the bedding plane.
$\beta_{\perp}$ is the S-wave velocity perpendicular to the bedding plane.
$\propto_{=}$ is the P-wave velocity parallel to the bedding plane and
$\beta_{=}$ is the S-wave velocity parallel to the bedding plane.
When the density, ρ of the sample is known, elastic stiffness constants, C_{11}, C_{33}, C_{44} and C_{66} are easily obtainable according to the Equations 7, 8, 9 and 10.
It is important to ensure a great coupling of the sample and the transducers to avoid air pockets between the transmitter and receiver transducers. To achieve this, a special coupling paste design for this purpose was smeared on the surface of the transducers before each test.

RESULTS AND DISCUSSION

Photomicroscopy of the shales studied (Figure 3) showed fractures and microcracks in the samples mainly along the bedding plane. X-Ray diffraction method is a good method widely used by researchers to investigate and characterize materials (Fakolujo et al. 2012; Dutrow and Clark, 2018 and Pandian, 2014). In this work, the X-Ray diffraction of the tested shales showed that SHL1 is comprised of Kaolinite, Illite, Montmorillonite, and Quartz minerals while SHL2 is comprised of Kaolinite, Illite and Quartz minerals (Figure 4).

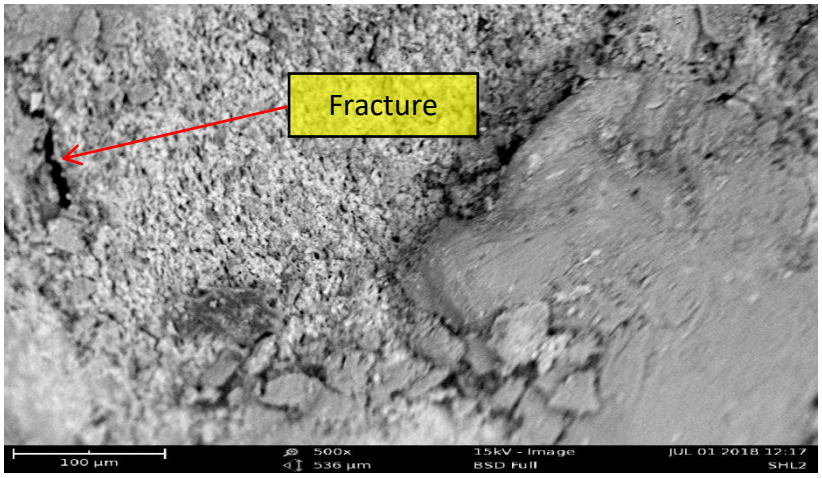

(a)

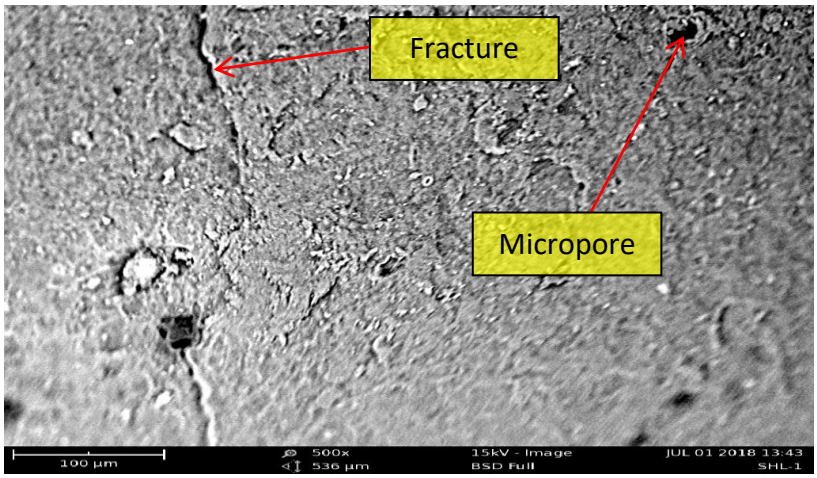

(b)

Figure 3: Photomicroscopy of (a) SHL1 and (b) SHL2

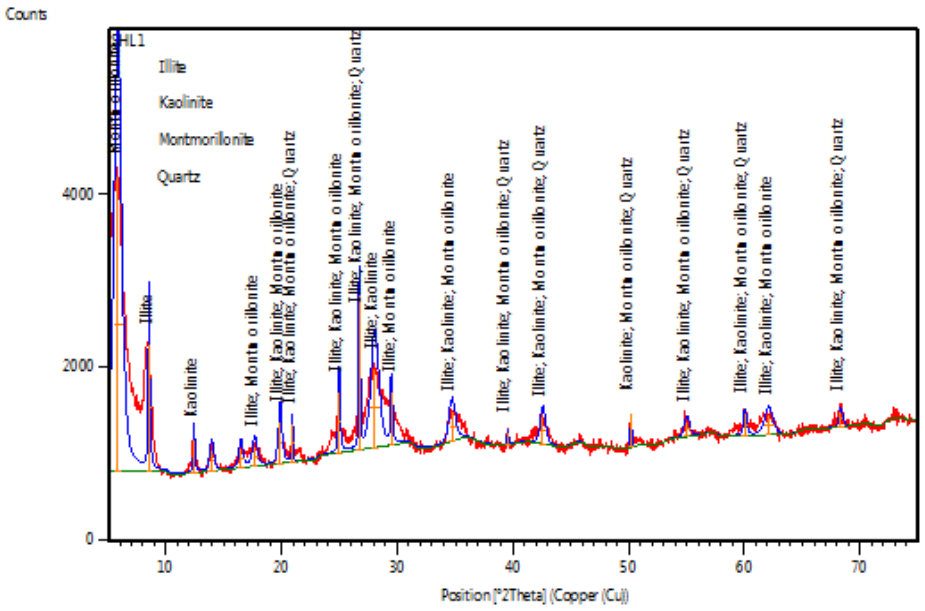

(a)

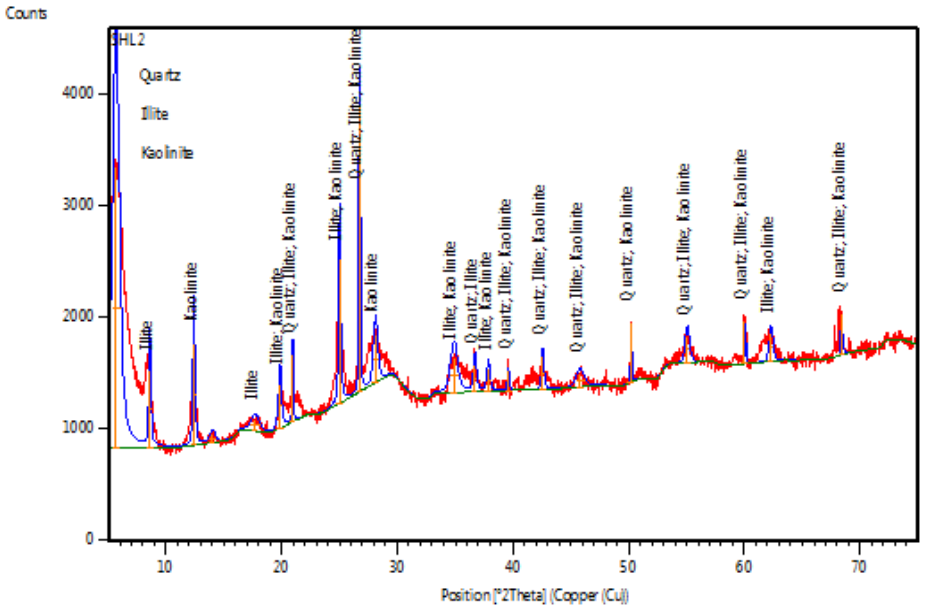

(b)

Figure 4: XRD Spectral of (a) SHL1 and (b) SHL2

Ultrasonic Velocities

Ultrasonic pulse transmission method had been used to determine the compressional and shear wave velocities in the shale samples. Compressional and shear wave velocities perpendicular and parallel to the bedding plane were measured and recorded. Tables 1 and 2 show the variations of the compressional and shear wave velocities of shales with temperature for both the vertical and horizontal plugs. Ultrasonic velocity measurement with transducer arrangement perpendicular to the bedding plane exhibited lower values relative to the velocity measurement along the bedding plane. Also, relatively large P and S wave velocity changes were exhibited in the velocity measurement perpendicular to the bedding plane in both samples. The velocities were large in SHL 1 than in SHL 2.

Table 1: Ultrasonic Velocities of SHL1 on the Vertical and Horizontal Plugs

Temperature (˚C)	Vertical Plug		Horizontal Plug	
	V_P (m/s)	V_S (m/s)	V_P (m/s)	V_S (m/s)
50	2998	1414	3566	1767
100	2961	1398	3534	1745
150	2946	1378	3480	1717
200	2884	1366	3440	1716
250	2819	1350	3420	1704
300	2756	1344	3407	1699

Table 2: Ultrasonic Velocities of SHL2 on the Vertical and Horizontal Plugs

Temperature (˚C)	Vertical Plug		Horizontal Plug	
	V_P (m/s)	V_S (m/s)	V_P (m/s)	V_S (m/s)
50	3024	1417	3625	1793
100	2987	1395	3580	1759
150	2913	1387	3560	1737
200	2849	1368	3554	1719
250	2763	1352	3501	1716
300	2715	1350	3469	1710

Velocity Ratio and Elastic modulus

Important parameters obtainable from the measured velocities include the velocity ratio and elastic modulus. Estimated values of the velocity ratio and elastic modulus are given respectively in Tables 3 and 4. The velocity ratio for both samples showed higher values in the vertical orientation of the bedding plane than in the horizontal direction. Meanwhile, the elastic modulus was higher in the horizontal plugging than in the vertical. This indicated that the rocks will resist deformation more along the bedding plane.

Table 3: Velocity ratio of shales at various temperatures for the Vertical and Horizontal Plugs

Temperature (˚C)	Velocity Ratio			
	SHL1		SHL2	
	Vertical Plug	Horizontal Plug	Vertical Plug	Horizontal Plug
50	2.12	2.02	2.13	2.12
100	2.12	2.03	2.14	2.12
150	2.14	2.03	2.10	2.12
200	2.11	2.00	2.08	2.11
250	2.09	2.01	2.04	2.09
300	2.05	2.01	2.01	2.04

Table 4: Elastic modulus of shales at various temperatures for the Vertical and Horizontal Plugs

Temperature (˚C)	Elastic modulus (GPa)			
	SHL1		SHL2	
	Vertical Plug	Horizontal Plug	Vertical Plug	Horizontal Plug
50	12.08	18.51	11.96	18.94
100	11.71	18.08	11.71	18.26
150	11.60	17.51	11.32	17.85
200	11.25	17.42	11.09	17.53
250	10.95	17.19	10.77	17.39
300	10.86	17.08	10.62	17.24

Stiffness Constants and Anisotropic Parameters

For an elastic material, the resistance of the body to deformation is known as the stiffness of the material, which is very important in rock studies like failure determination and wellbore stability analysis of rocks. When the stiffness constants are determined, they can be used to obtain Thompson's anisotropic parameters. The stiffness constants and anisotropic parameters of SHL1 and SHL2 are given in Tables 5 and 6 respectively. The parameters reflected the heterogeneity of the rocks as they reduce with increasing temperature. For SHL1 and SHL2, the values of the parameter (at the same temperature) were observed to be very close.

Table 5: Temperature and Stiffness constants of SHL 1

Temperature (C)	Stiffness constants SHL 1			
	C_{11} (GPa)	C_{33} (GPa)	C_{44} (GPa)	C_{66} (GPa)
50	28.19	19.93	4.45	6.92
100	27.69	19.44	4.31	6.75
150	26.85	19.24	4.26	6.54
200	26.24	18.44	4.15	6.53
250	25.93	17.62	4.05	6.44
300	25.73	16.84	4.04	6.40

Table 6: Temperature and Stiffness constants of SHL 2

Temperature (C)	Stiffness constants SHL 2			
	C_{11} (GPa)	C_{33} (GPa)	C_{44} (GPa)	C_{66} (GPa)
50	28.92	20.13	4.40	7.08
100	28.21	19.64	4.30	6.81
150	27.89	18.68	4.18	6.64
200	27.80	17.87	4.11	6.50
250	26.98	16.80	4.01	6.48
300	26.49	16.22	3.98	6.44

Effect of temperature on Anisotropic Parameters of the Samples

The trends of variation of the anisotropic parameters with temperature were studied and were shown in Figure 5 and Table 7. At lower temperatures, both anisotropic constants (Ɛ and ϒ) exhibited average constant values. The parameters however showed a noticeable increase with increased temperature from about 150 ˚C. For the two samples studied, gamma exhibited a higher increasing rate than epsilon such that the two constants were converging as the temperature increased.

Table 7: Anisotropic constants of shales at various temperatures

Temperature (˚C)	Anisotropic Constants							
	SHL1				SHL2			
	α (m/s)	β (m/s)	ϒ	Ɛ	α (m/s)	β (m/s)	ϒ	Ɛ
50	3024	1414	0.304	0.218	2998	1411	0.278	0.207
100	2987	1398	0.297	0.218	2976	1400	0.282	0.205
150	2963	1378	0.304	0.222	2946	1387	0.286	0.207
200	2938	1366	0.301	0.232	2918	1368	0.285	0.211
250	2907	1350	0.308	0.225	2890	1352	0.287	0.210
300	2885	1330	0.323	0.223	2871	1332	0.295	0.204

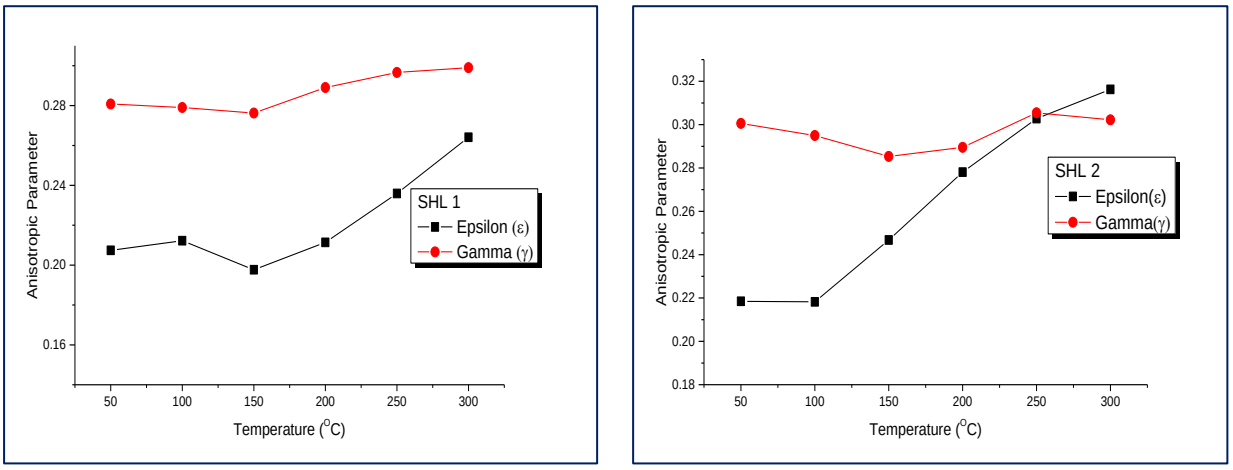

(a) (b)

Figure 5: Variation of Anisotropic constants of (a) SHL1 and (b) SHL 2 with Temperature

Effect of Anisotropic Parameter on Poisson's ratio and Elastic Modulus

The relationship between the Thompson anisotropic parameters and Poisson's ratio as well as the relationship between the anisotropic parameters and elastic modulus of the sample was investigated. The experimental observation showed a notable reduction in the Poisson's ratio with increasing Thompson anisotropic parameters, Epsilon and Gamma. The reduction in the Poisson's ratio is more notable in the vertical orientation of the bedding plane. This observation indicated the effect of fractures and microcracks parallel to the bedding plane. The behavior occurred both in SHL 1and SHL 2 (Figure 6). Also with the anisotropic parameters, elastic modulus exhibited an inverse relationship (with very small change) (Figure 7). The observation showed the same trend for both vertical and horizontal orientations of the bedding plane (the elastic modulus is higher in the vertical orientation than in the horizontal). The observed relationship of the anisotropic parameter with the Poisson's ratio and elastic modulus indicated that the microcracks along the bedding plane gradually close up as the samples expand with increasing temperature - a behavior that is capable of increasing the tendency of higher elastic property in the vertical orientation of the bedding plane of the shales.

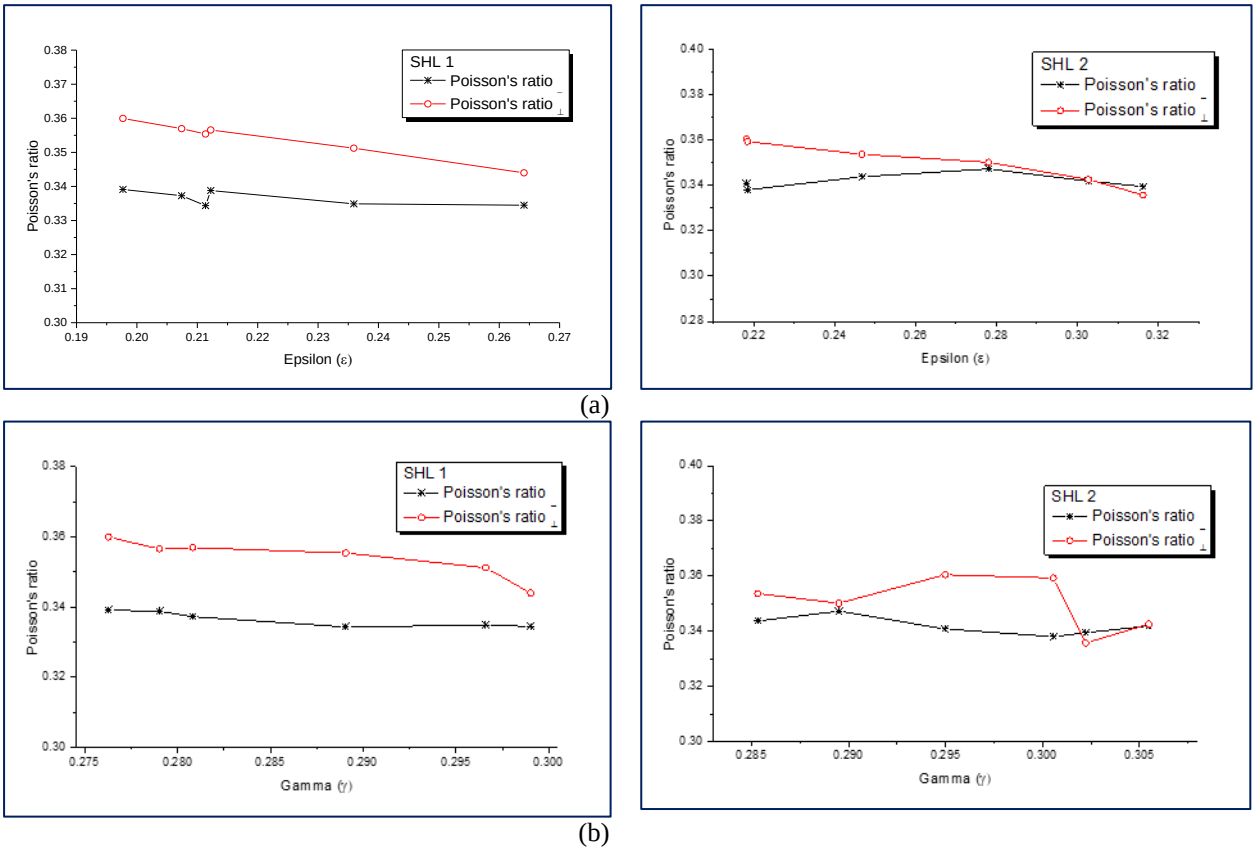

Figure 6: Variation of Poisson's ratio of SHL1 and SHL 2 with (a) Epsilon and (b) Gamma

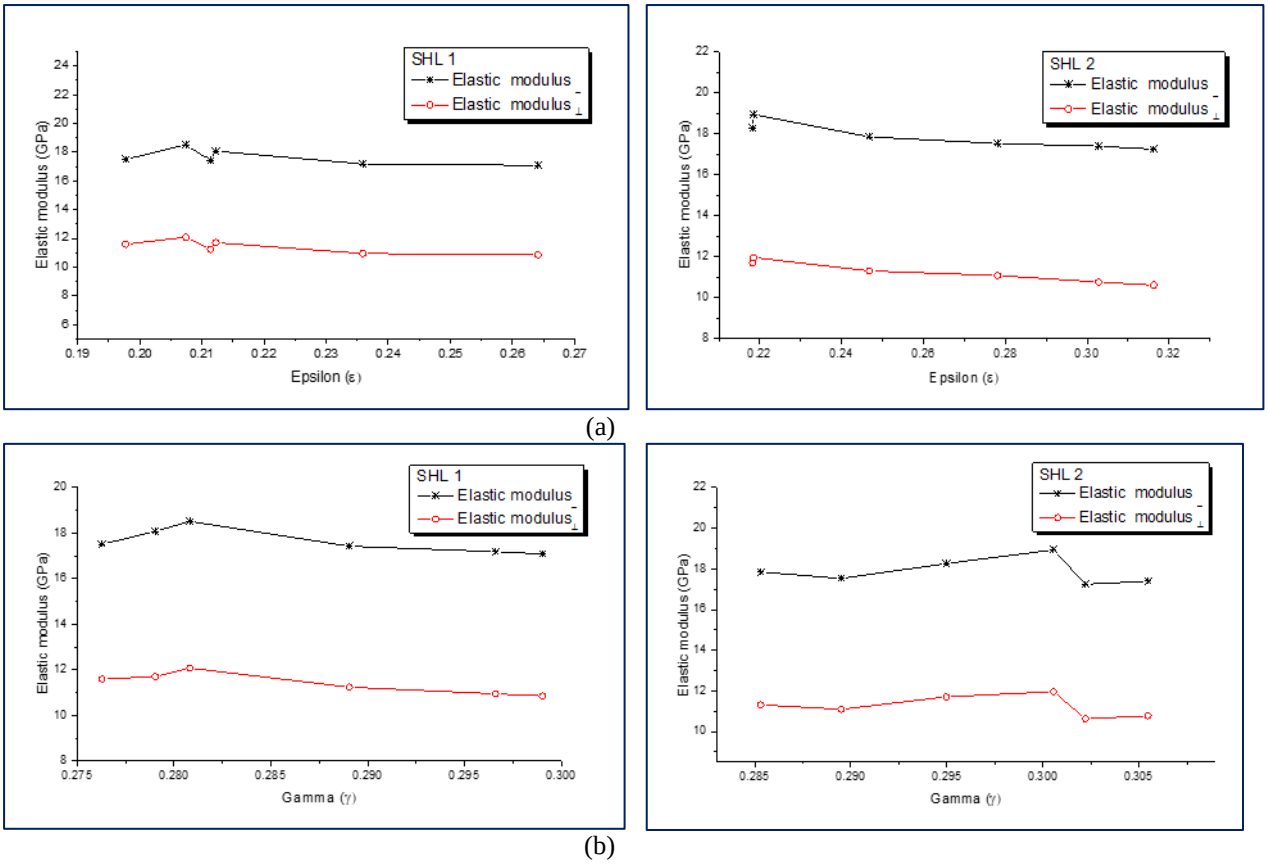

Figure 7: Variation of Elastic modulus of SHL1 and SHL 2 with (a) Epsilon and (b) Gamma

CONCLUSION

Effect of temperature on the Thompson anisotropic parameters of shales have been experimentally investigated in the study area, Ogun State southwestern Nigeria. The study showed that the shale from the study area exhibited elastic anisotropic behavior. Both compressional and shear wave velocities exhibited an inverse relationship with temperature as the velocities decreased with increasing temperature in all orientations of the bedding plane while the anisotropic parameters, Gamma (ϒ) and Epsilon (Ɛ) were directly related to the temperature. The result showed that there were fractures and microcracks along the bedding plane of the shales, which tend to close up as the samples expand due to temperature increase. The result of the experiment also showed that Poisson's ratio and elastic modulus of the samples reduced very slightly with increasing Epsilon and Gamma.

REFERENCES

Ahmadov R., Vanorio T. and Mavko G. (2009). Confocal laser scanning and atomic force microscopy in estimation of elastic properties of the organic-rich Bazhenov Formation: The Leading Edge, 28, 18– 23, doi: 10.1190/1.3064141

Anil S. and Anirbid S. (2014) Sources and Measurement of Velocity Anisotropy of Cambay Shale, Cambay Basin, India. IJLTEMAS 3(5) 169

Baoping L. and Hongzhi B. (2005) "Advances in calculation methods for rock mechanics parameters," *Petroleum Drilling Techniques*, 33(5): 44–47

Brahma J., and Sircar A. (2014). Estimation of the Effect of Anisotropy on Young's Moduli and Poisson's Ratios of Sedimentary Rocks Using Core Samples in Western and Central Part of Tripura, India International Journal of Geosciences, 5: 184-195

Dewhurst D. N. and Siggins A. F. (2006) Impact of fabric, microcracks and stress field on shale anisotropy. *Geophys. J. Int.* 165, 135–148. doi: 10.1111/j.1365-246X.2006.02834.x

Domnesteanu, P., McCann, C. and Sothcott, J. (2002). Velocity anisotropy and attenuation of shale in under- and overpressured conditions, *Geophys. Prospect.*, 50, 487–503.

Douma L.A.N.R. Houben M.E. Primarini M. I. W. and Barnhoorn A. (2016) The Effect of Temperature and

Pressure on the Rock Mechanical Behaviour of the Whitby Mudstone Formation, UK. Fifth EAGE Shale Workshop 2-4 May 2016, Catania, Italy

Dutrow BL and Clark CM (2016) X-ray powder diffraction (XRD). Geochemical instrumentation and analysis, slideshare.net. https:// www. slide share. net/ Sumit Tiwar i69/ xrayp owder- diffraction- xrd

Fakolujo O. S., Olokode O. S., Aiyedun P. O., Oyeleke Y. T. and Anyanwu B. U. (2012) Studies on the five (5) selected clays in Abeokuta, Nigeria. Pacific J Sci Technol 13(1):83–90

Hornby B. E. (1998). Experimental laboratory determination of the dynamic elastic properties of wet, drained shales, *J. Geophys. Res.*, 103/B12, 29 945–964.

Huang S. L., Speck R. C. and Wang Z. (1995). The temperature effect on swelling of shales under cyclic wetting and drying. Int. J. Rock Mech. Min. Sci. & Geomech. Abstr. *32(3), 227–236.* doi:10.1016/0148-9062(94)00044-4

Jakobsen, M. & Johansen, T.A. (2000). Anisotropic approximations for mudrocks: a seismic laboratory study, *Geophysics*, 65, 1711–1725.

Ji-Xin D., Ge S., Xun-Rui L., and Jun Y. (2004). Analysis of the velocity anisotropy and its causative Factors in shales and mudstones. *Chinese journal of Geophysics*, 47:972-979, University of Petroleum, Beijing, China, 2004

Johnston D. H. (1987). Physical properties of shale at temperature and pressure Geophysics. 52(10): 1391 – 1401

Johnston, J. E. and Christensen N. I. (1995) Seismic anisotropy of shales. J. Geophys. Res., B4, 5991-6003.

Kuforiji H. I., Olurin O. T., Akinyemi O. D. and Idowu O. A. 2021. Wave Velocity Variation with Temperature: Influential Properties of Temperature Coefficient ($\partial V/\partial T$) of Selected Rocks. Environmental Earth Sciences, 80 (638) DOI: 10.1007/s12665-021-09937-4

Kumar V., Sondergeld C. H. and Rai C. S. (2012). Nano to macro mechanical characterization of shale: Presented at SPE Annual Technical Conference and Exhibition, SPE 159804

Okeke O. C. and Okogbue C. O. (2011). Shales: A review of their classifications, properties and importance to the petroleum industry. Global Journal of Geological Sciences. 9(1); 55-73

Okosun E. A. (1989) Eocene ostracoda from Oshosun formation Southwestern Nigeria, Journal of African Earth Sciences (and the Middle East). 9(3 – 4): 669 – 676

Pandian MS (2014) X-ray diffraction analysis: principle, instrument, and applications. Researchgate samples by X-ray diffraction: discussion. Am Miner 72:438–440

Petters S. W. and Olsson R. K. (1979) Planktonic Foraminifera from the Ewekoro Type Section (Paleocene) Nigeria. *Micropaleontology*, 25(2): 206-213

Proceq (2011) Operating Instructions Pundit Lab / Pundit Lab+ Ultrasonic Instrument.
Shales Under Cyclic Wetting and Drying. *Int. J. Rock Mech. Min. Sci. & Geomech. Abstr*. 32(3): 227-236, 1995

Sondergeld C. H. and Rai C. S. (1993) A new exploration tool: Quantitative core characterization: PAGEOPH, 213/4, 249-268.

Sondergeld C. H., Rai C. S. Margesson R. W. and.Whidden K. J. (2000) Ultrasonic measurement of anisotropy on the Kimmeridge shale: 70th Annual International Meeting, SEG, Expanded Abstracts, 1858–1861

Sone H. and Zoback D. (2013) Mechanical properties of shale-gas reservoir rocks – Part 1: Static and dynamic elastic properties and anisotropy. Geophysics. 78(2)

Takanashi M., Nishizawa O. Kanagawa K. and Yasunaga K. (2001). Laboratory measurements of elastic anisotropy parameters for the exposed crustal rocks from the Hidaka Metamorphic Belt, Central Hokkaido, Japan. Geophys. J. Int. 145, 33–47

Thomsen, L., (1986). Weak elastic anisotropy, *Geophysics*, .51:1954-1966

Tosoya, C, and Nur, A., 1982, Effects of diagenesis and clays on compressional velocities in rocks: Geophysics. Res. Lett., 9, 5-8.

Vernik L. and Liu X. (1997). Velocity anisotropy in shales: A petrophysical study. *Geophysics* 62(2): 521-532

Vernik L. and Milovac J. (2011). Rock physics of organic shales: The Leading Edge, 30, 318–323, doi: 10.1190/1.3567263

Wang Y. and Li C.H. (2017) Investigation of the P- and S-wave velocity anisotropy of a Longmaxi formation shale by real-time ultrasonic and mechanical experiments under uniaxial deformation. *Journal of Petroleum Science and Engineering* 158 (2017): 253 – 257.

Waxman, M. H. and Thomas, E. C, (1974) Electrical conductivities in shaly sands-I. The relation between hydrocarbon saturation and resistivity index; II. The temperature coefficient of electrical conductivity: J. Petr. Tech., Trans. Am. Inst. Min. Metall. Petro Eng., 257,213-255.

Xu F., Yang C. Guo Y. Wang L. Hou Z. Li H. Hu X. and Wang T. (2017). Effect of bedding planes on wave velocity and AE characteristics of the Longmaxi shale in China. *Arab J Geosciences* 10:141. DOI 10.1007/s12517-017-2943-y

Xu H., Zhou W., Xie R., Da L., Xiao C., Shan Y. and Zhang H. (2016) Characterisation of Rock Mechanical Properties Using Lab Tests and Numerical Interpretation Model of Well Logs. Mathematical Problems in Engineering Volume 2016, Article ID 5967159, 13 pages doi.org/10.1155/2016/5967159